

# The Influence of Self-Compacting Steel Fibre Reinforced Concrete Infill on the Flexural Strength and Ductility of Masonry Walls

by

LUIZ A. P. de OLIVEIRA and LUIS F. A. BERNARDO

e-mail: [luiz.oliveira@ubi.pt](mailto:luiz.oliveira@ubi.pt), [luiz.bernardo@ubi.pt](mailto:luiz.bernardo@ubi.pt)

Civil Engineering and Architecture Department, University of Beira Interior - Covilhã – Portugal

## ABSTRACT

*This paper presents an experimental study on the influence of longitudinal reinforcement ratio and steel fibre volume in self-compacting concrete infill on the strength and ductility of reinforced masonry walls subjected to flexure. Flexure tests were performed as four-point bending tests on twelve walls. The analysis of the concrete infill contribution to the walls capacity is made considering recent recommendations for steel fibre reinforced concrete design. A ductility index was defined and applied to study the ductility behaviour of the masonry walls. The analysed variables are the longitudinal reinforcement ratio and the steel fibre volume in the concrete infill.*

## 1. INTRODUCTION

In a typical reinforced hollow unit masonry construction, the steel reinforcing provides a strong structure that can be tied together and better resist the lateral dynamic forces of wind and earthquakes. The difficulty in consolidating the concrete infill by vibration requires that this material must be fluid enough to fill all voids in the hollow unit masonry space and to completely encase the reinforcement. To assure the necessary consolidation between a hollow unit and reinforcement, in practice, the low lift filling method instead of high lift method is chosen to fill the vertical cells in the masonry. This choice increases the duration of wall construction. In order to get round these difficulties, the concrete infill must be self-compacting.

Steel fibre reinforced concrete (SFRC) has been successfully used in various types of construction due to the fact that adding steel fibres improves the durability and mechanical properties of hardened concrete, notably flexural strength, toughness, impact strength, resistance to fatigue, vulnerability to cracking and spalling [1]. However, the addition of steel fibres also reduces the workability of fresh concrete; hence the use of SFRC as concrete infill is inappropriate.

Self-compacting concrete has recently been successfully developed by several authors [2,3]. In addition to its high workability and higher mechanical properties compared with normal strength concrete, self-compacting concrete reduces the energy, expense and time required for consolidation at the construction site. Steel fibre reinforcement self-compacting concrete (SFRSCC) feasibility has been recently observed in some investigation works, such as those by AMBROISE *et al.* in 1999 [4], GROTH and THUN in 2000 [5], GRÜNEWALD and WALRAVEN in 2001 [6] and OLIVEIRA *et al.* in 2003 [7]. Knowledge of the mechanical performance at the ultimate state and the influence of fibre volume on SFRSCC strengthened masonry walls is extremely scarce because of its very recent development [8].

For reinforced masonry structures built with hollow concrete blocks, the use of SFRSCC to fill the masonry voids could allow the substitution and/or the reduction of the masonry reinforcement without any decrease in structural performance. On the other hand, the application of SFRSCC finds its place not only in masonry wall reinforcements, built according to the EN 1996-1-1 [9], but also in its retrofit to ancient masonry. It is therefore important to know the behaviour of the masonry walls (reinforced or not) when consolidated with steel fibre concrete infill, mainly for the ultimate strength capacity and final deformation of the compression areas. This last aspect is very important to assure a wall's ductile behaviour.

Generally, ductility may be defined as the capacity of a material, section, structural element or even a complete structure to be subjected to an excessive plastic deformation without high load-bearing capacity loss. This property is very important because it is directly related to the capacity of stress redistribution and structural safety. It must therefore always be considered in reinforced masonry design.

It is well known that ductile structural elements show advance signs of incapacity, such as high deformation and large cracks, before structural collapse. This period may be crucial to minimize, or even to avoid, great material damage and/or human victims in situations of high structural demands, a typical example being an earthquake. Moreover, the ductility of structural elements leads also to the possibility of gradual stress redistribution, avoiding in this way any sudden transmission of stress from critical sections to other element sections which in turn might lead to a progressive structural collapse. The earlier statement justifies the importance now attributed to the ductility of structural elements.

So, the study of the behaviour of masonry walls strengthened with SFRSCC, in terms of strength and ductility, needs to be completed before this strengthening solution may be reliably used on this kind of structural element. This is possible since the properties of steel fibre reinforced concrete infill have been studied sufficiently to give the desired workability necessary to attain self-compactability.

## 2. DESCRIPTION OF THE EXPERIMENTAL WORK

### 2.1 Materials

#### 2.1.1 Masonry units

Masonry walls were built with hollow concrete blocks with nominal dimensions of 200 x 200 x 400mm (Figure 1), whose characteristics were obtained according to European standards [10,11]. The average compressive strength of hollow concrete blocks obtained from 6 test specimens was 10.2N/mm<sup>2</sup> and water absorption was 5.1%.



**Figure 1 Hollow concrete blocks**

### 2.1.2 Mortar

The most important mortar function is to bind the masonry units and make the masonry joints watertight. For mortar under flexural behaviour a small significant structural function has been considered. For that reason, only one mortar composition was used in this study. The mortar unit volume proportions 1.0 : 0.1 : 3.5 (cement : hydrated lime : sand) was used to lay the masonry units of all the walls tested. The compressive strength mortar tests were made according to EN 1015-11 [12] and analyzed according to EC6 [9].

An average compressive strength of  $8.5\text{N/mm}^2$  was obtained based on 9 test specimens. The mortar is thus strength class M5 that is the minimum strength class required of masonry cement mortars [9].

### 2.1.3 SFRSCC

The SFRSCC mix was optimised for mortar content in order to ensure the involvement of coarse aggregates and fibres, as well as to provide the concrete filling capacity. This will ensure an adequate consolidation of the wall reinforcement when it is poured in without compaction [7]. A Portland cement type II/B-L 32.5 and a fly ash from a thermoelectric power station were used as binder materials. A super-plasticizer based on modified carboxylates (ViscoCrete 3000 from SIKA) was used to attain a suitable plastic viscosity. The maximum super-plasticizer content compatible with the cement used is 3.0%.

Two types of fine aggregate (sand with maximum sizes of 1.19mm and 4.76mm, respectively) and of coarse aggregate (granite crushed stone with maximum sizes of 9.52mm and 19.10mm, respectively) were used in the concrete infill composition. The mixture of fine aggregates was made with 50% of each type of sand. The coarse aggregate was composed of 70% of 9.5mm maximum size crushed stone and 30% of 19mm maximum size crushed stone.

Steel fibres with hooked ends (Figure 2) with a commercial designation of DRAMIX ZP 306 [13] were used. The fibres' aspect ratio is  $l_f / d_f = 48$ , where  $l_f$  is the fibre length and  $d_f$  is the fibre diameter. This value was chosen by taking into account the hollow unit masonry void space (110 x 110mm) and to assure no concrete infill blocking problems. The steel fibre yield strength is approximately  $1100\text{N/mm}^2$ . No fibre segregation was observed in any of the concrete batches.

The SFRSCC workability evaluation was based on three methods largely used in the self-compacting research field: Slump-Flow, L Box and V Funnel Tests.

The compressive strength of the hardened SFRSCC was obtained from 150mm cubic specimens, according to NP EN 12390-3 [14]. The flexural strength of SFRSCC was obtained by 3-point load tests on beams with a cross section of 100 x 100mm, simply supported with a span of 450mm,

according to the recommendations of RILEM TC 162-TDF [15].

Four concrete mixture-solutions from SFRSCC mix design with the proportions shown in Table 1 were used in this study. In the third table column, the optimum mortar ratio (Mort.) to attain the slump-flow values is reported. This characterises the concrete self-compactability, as well as the corresponding values of  $(l_f/d_f) \cdot V_f$  relative to the fibre index, where  $V_f$  is the volume of fibres. The mortar ratio is the mortar mass (cement + sand) percentage in the concrete infill.

It was observed that all mixtures were self-compactable even with the highest addition of steel fibres, that is, 120kg of steel fibres per cubic meter of concrete ( $V_f = 1.5\%$ ).

The results of hardened SFRSCC tests are presented in Table 2. These include the 28 days compressive strength ( $f_c$ ) obtained for six test specimens and average values of the equivalent flexural strength ( $f_{eq,2}$  and  $f_{eq,3}$ ) obtained from 3 test specimens for each mixture, according to the recommendations of RILEM TC 162-TDF [16].

Figure 3 shows some typical force (P) – mid-span deflection ( $\delta$ ) curves obtained from SFRSCC flexural strength tests. Figure 3 clearly shows the influence of steel fibre volume in the performance of the mixtures.

### 2.1.4 Masonry wall reinforcement

Hot-rolled steel ribbed bars, Class S400, were used as wall longitudinal reinforcement. The bars were placed in the centre of the hollow block. The diameters of the bars used as reinforcement were 8, 10 and 16mm. Tensile tests were carried out to obtain the yield tensile strength ( $f_{ym}$ ), first yield strain ( $\epsilon_{ym}$ ) and maximum tensile strength ( $f_{tm}$ ). The results for tensile tests are presented in Table 3.

## 2.2 Masonry walls

Figure 4 shows a schematic representation of the geometric characteristics of the twelve walls tested. The wall dimensions were: length = 1.400m; width = 1.000m; thickness = 0.200m. The experimental variables are the longitudinal reinforcement ratio and the steel fibre volume in the SFRSCC. The walls were divided into 3 series with the following characteristics:

- series W 08: 4 walls with minimum reinforcement [9] and with 3 bars of 8mm diameter ( $A_s = 1.51\text{cm}^2$ );
- series W 10: 4 walls with optimised reinforcement (balanced failure criterion) and with 3 bars of 10mm diameter ( $A_s = 2.36\text{cm}^2$ );
- series W 16: 4 walls with reinforcement for strain  $\epsilon_{syd} = 1.66\text{‰}$  (brittle failure criterion) and with 3 bars of 16mm diameter ( $A_s = 6.03\text{cm}^2$ ).

Each wall series was built with the mixtures reported in Table 1.



Figure 2 Hooked steel fibres

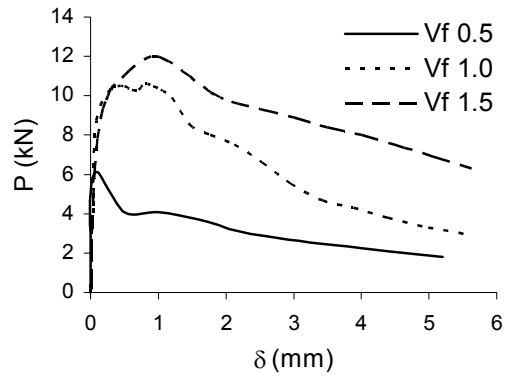


Figure 3 P - δ curves for SFRSCC

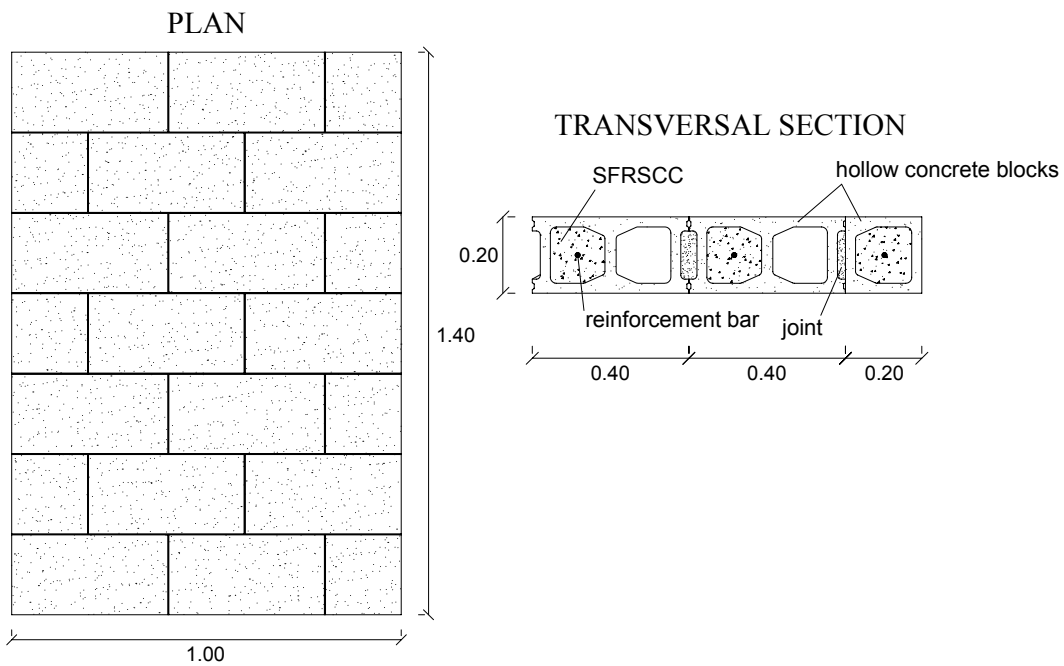


Figure 4 Details of tested walls

Table 1  
Mixture compositions and fresh properties

Mass proportions (c:fa:s:a) <sup>(1)</sup>	V <sub>f</sub> <sup>(2)</sup> (%)	SP <sup>(3)</sup> (%)	Mort <sup>(4)</sup> (%)	(l <sub>f</sub> / d <sub>f</sub> ).V <sub>f</sub> (%)	Slump flow <sup>(5)</sup>		L Box <sup>(5)</sup> H <sub>2</sub> / H <sub>1</sub>	V Funnel <sup>(5)</sup> Time (sec)
					D <sub>final</sub> (mm)	T <sub>500</sub> (sec)		
A – 1:0.15:1.78:1.72 w/cm = 0.40	0	2.0	63	0	765	1'00"	0.88	2'73"
B – 1:0.15:2.00:1.50 w/cm = 0.40	0.5	2.5	68	34.5	735	1'38"	1.00	3'22"
C – 1:0.30:2.06:1.44 w/cm = 0.40	1.0	2.5	70	69.0	730	1'85"	1.00	4'02"
D – 1:0.50:2.15:1.35 w/cm = 0.40	1.5	2.5	73	103.6	760	1'02"	0.90	3'36"

<sup>(1)</sup> c = cement; fa = fly ash; s = sand; a = coarse aggregate (19 mm); w = water; cm = cementitious materials;

<sup>(2)</sup> V<sub>f</sub> = fibre volume; <sup>(3)</sup> SP = superplasticizer; <sup>(4)</sup> Mort = mortar ratio.

<sup>(5)</sup> in accordance with The "European Guidelines for Self Compacting Concrete"

**Table 2**  
**Compressive and equivalent flexural strength**

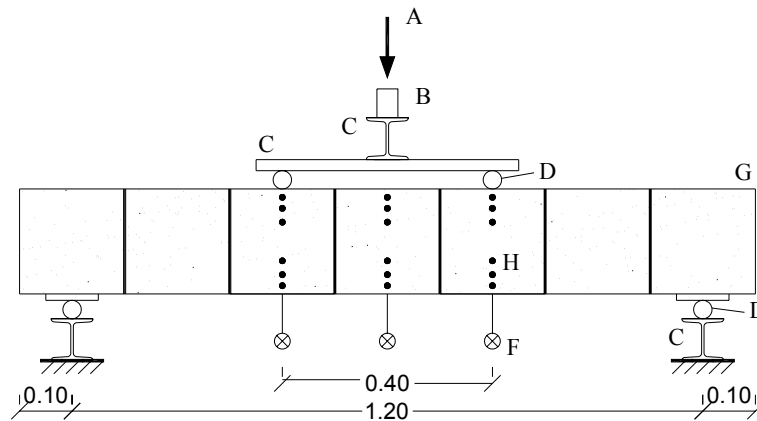
Mixture	$V_f$ (%)	$f_c$ (N/mm <sup>2</sup> )	$f_{eq,2}$ (N/mm <sup>2</sup> )	$f_{eq,3}$ (N/mm <sup>2</sup> )
A	0	28.0	-	-
B	0.5	28.0	2.98	2.51
C	1.0	26.0	6.48	5.84
D	1.5	27.0	12.12	6.97

**Table 3**  
**Experimental results of tested steel bar reinforcement**

Diameter (mm)	$f_{ym}$ (N/mm <sup>2</sup> )	$\epsilon_{ym}$ ( $\times 10^{-6}$ )	$f_{tm}$ (N/mm <sup>2</sup> )
$\phi 8$	530	2650	640
$\phi 10$	534	2672	642
$\phi 16$	575	2876	679



**Figure 5 Transverse section of tested walls**



A – Applied Load; B – Load Cell; C – Steel Plate/Beam; D – Roller Support;  
F – Displacement Transducer; G – Wall Test; H – Demec targets

**Figure 6 Typical set-up for testing wall specimen**

Figure 5 shows the reinforcement bars located in the masonry wall. The reinforcement bars were placed in the hollow centre. Then the effective depth is constant with a value of 100mm.

The walls tested were supported simply at the ends and were subjected to a symmetrical load composed by two equal concentrated forces, applied at approximately

one-thirds of the span. The purpose of this loading was to obtain a central region, between the applied forces, subjected to pure bending, without the influence of shear.

Figure 6 shows a schematic representation of the wall specimen in its test position and the location of the external measuring instruments used in this study.

The main load was applied through a hydraulic jack and was measured by means of load cells. The vertical displacements at mid span and under the load points of the wall were measured by displacement transducers. The strains were also measured along the height of the wall section in the central zone (between the point loads). For this purpose, an external grid of Demec target measuring points was stuck to one lateral face of the walls. Resistance strain gauges were fixed to the longitudinal tensile reinforcement in the mid span to measure the evolution of strains of the steel bars during the test. All the readings from the measuring instruments were recorded on data logger acquisition equipment.

Figure 7 shows one of the test walls in the test frame. Figure 8 shows the failure section (central zone) of the previous wall at the end of the test. All the walls failed in pure bending in the central zone (between load application points) in a masonry joint section.

### 3. EVALUATION OF THE WALL BENDING CAPACITY

#### 3.1 Theoretical analysis of SFRSCC contribution to the bending moment of resistance

The analysis presented in this section is intended to estimate the theoretical bending moment of resistance of the

walls considering the steel fibres reinforced concrete infill contribution. RILEM TC 162 – TDF published some design recommendations for steel fibres reinforced concrete [15-17]. The flexural model recommended by this design method is shown in Figure 9. The flexural design model for steel fibre reinforced concrete based on the simplified rectangular block stress diagram (Figure 10) was proposed by VANDERWALLE in 1994 [18]. Using this simplified model, the theoretical bending moment of resistance was calculated for the reinforced walls filled with SFRSCC made with different fibre concentrations.

The equivalent flexural strength, which is an important parameter to characterize the post-cracking behaviour of the steel fibre reinforced concrete, is considered in this study as a contributor to the reinforced masonry wall capacity. The theoretical bending moment of resistance ( $M_{R,theor}$ ) of the twelve walls is shown in Table 4. For the calculation of the resistance the average material strengths reported in Section 2.1 were employed. The analysis of the theoretical resistance of the walls shows that the fibres' contribution to the bending moment of resistance ( $M_{R,theor}$ ), expressed by the ratio  $M_{R,theor,n\%} / M_{R,theor,0\%}$  ( $n$  is the steel fibre volume in the concrete infill), becomes less important as the steel ratio increases.

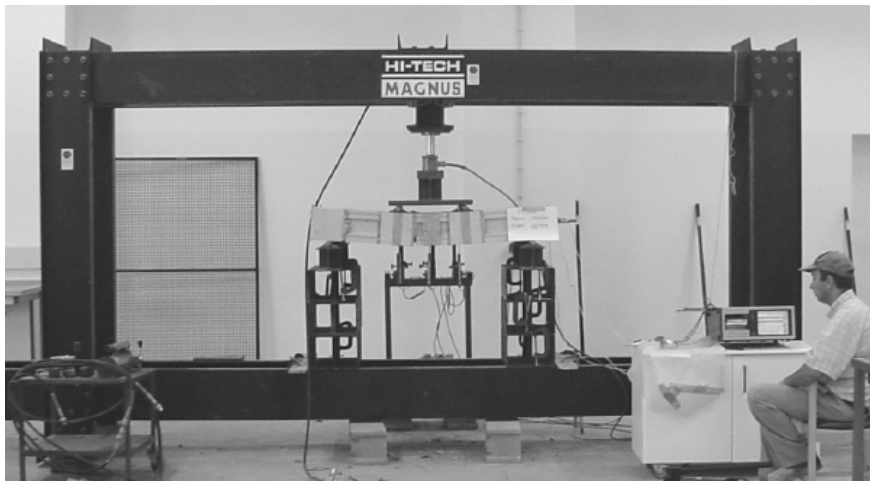


Figure 7 Wall specimen in test frame



Figure 8 Typical wall failure

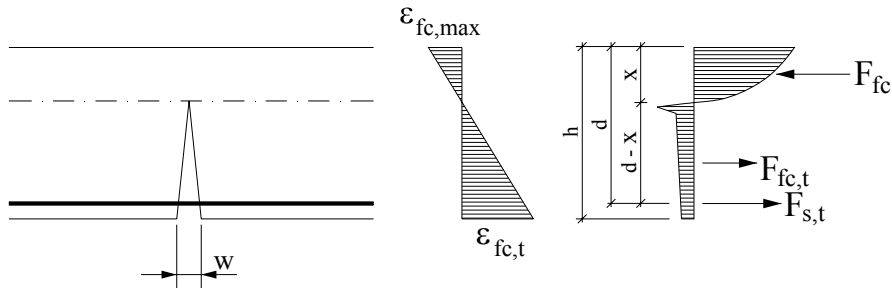


Figure 9 Flexural model for fibre reinforced concrete [15-17]

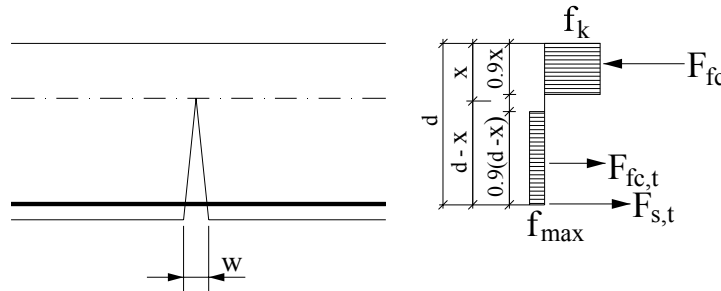


Figure 10 Simplified flexural model for fibre reinforced concrete [18]

Table 4  
Theoretical and experimental results for bending moments of resistance

Wall	$A_s$ (mm <sup>2</sup> )	$V_f$ (%)	$M_{R,theor}$ (kN.cm)	$\frac{M_{R,theor,n\%}}{M_{R,theor,0\%}}$	$M_{R,exp}$ (kN.cm)	$\frac{M_{R,exp}}{M_{R,theor}}$	$\frac{M_{R,exp,n\%}}{M_{R,exp,0\%}}$
W 08	150	0	466.0	1.00	733.8	1.57	1.00
		0.5	673.0	1.44	836.6	1.24	1.14
		1.0	890.0	1.91	1089.0	1.22	1.48
		1.5	953.0	2.05	986.0	1.03	1.34
W 10	236	0	679.0	1.00	1192.8	1.76	1.00
		0.5	848.0	1.25	1411.0	1.66	1.18
		1.0	1026.0	1.51	1507.2	1.47	1.26
		1.5	1076.0	1.58	1490.6	1.39	1.25
W 16	603	0	1175.0	1.00	2778.8	2.36	1.00
		0.5	1220.0	1.04	3183.8	2.61	1.15
		1.0	1268.0	1.08	2820.0	2.22	1.01
		1.5	1285.0	1.09	2835.2	2.21	1.02

### 3.2 Comparative analysis with experimental results

Figures 11, 12 and 13 show Load (P) – Deflection ( $\delta$ ) curves from the experimental readings recorded during the tests. P is related to the total applied load level and  $\delta$  to the deflection at mid-span of the walls.

The experimental values of the bending moments of resistance ( $M_{R,exp}$ ) for the twelve tested walls are reported in Table 4. The analysis of the results shows that the theoretical values of the resistance are safe, that there is a good agreement between the theoretical and the experimental tendencies and that all results show the steel fibres' contribution to the bending capacity of the walls.

These results validate the contribution of the fibres' tensile strength in the flexural walls behaviour. The increase of the wall flexural strength, when the theoretical failure occurs by steel bar reinforcement, such as for walls W 08 and W 10, is about 25% to 105%, depending of the steel fibre volume incorporated in the concrete infill.

## 4. DUCTILITY ANALYSIS

### 4.1 Definition and calculation of the ductility index

According to SHIN et al. [19], ductility is most clearly stated if its study is based on the deformation state of the element

being studied. The following parameters should be considered:  $x_u$  and  $x_y$ . The first one represents the deformation state of the element at the ultimate stage (ultimate value), while the second represents the deformation state for the load corresponding to the yielding of the steel reinforcement (yield value). Based on these two parameters, it is possible to define a ductility index as follows:  $\mu = x_u/x_y$ . This index allows the plateau of inelastic deformation of the element to be quantified, a result that is directly related to the ductility.

Based on the definition of ductility given earlier, a deflection ductility index ( $\mu_\delta$ ) (related to the recorded deflection at mid-span) is defined as the quotient between the deflection corresponding to the ultimate load ( $\delta_u$ ) and the deflection corresponding to the yielding load ( $\delta_y$ ):  $\mu_\delta = \delta_u / \delta_y$ .

When calculating the deflection ductility index, it is not easy to identify the point corresponding to the ultimate load in the experimental curves shown in Figures 11 to 13. This difficulty was extensively discussed by BERNARDO and LOPES in 2003 [20]. To make a comparative analysis between structural elements of a same study, those authors used a criterion to quantify a "conventional" ultimate value. To define the ultimate point on the behaviour curve, the criterion used was that of making the ultimate point on the behaviour curve corresponding with the point of intersection

between the final part of the curve and a horizontal line across the point where the reinforcement starts to yield. If no intersection is found to occur between the aforementioned line and the behaviour plot, the ultimate point is simply ascribed to the ultimate point on the curve. This methodology is valid for comparative purpose among all the walls tested. This criterion was used for the study described in this paper.

Table 5 presents the ultimate and the yielding values of the load ( $P_u$  and  $P_y$ ) and of the deflection ( $\delta_u$  and  $\delta_y$ ) obtained from  $P - \delta$  curves. The yielding load was calculated using experimental records of the strains in the longitudinal tensile reinforcement. These values were compared with the reference values obtained in the tensile tests on the steel specimens (average values for yield strains).

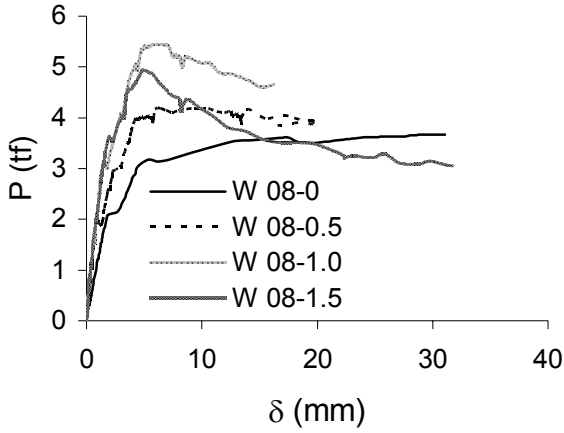


Figure 11 Load (P) – Deflection ( $\delta$ ) Curves (Series W 08)

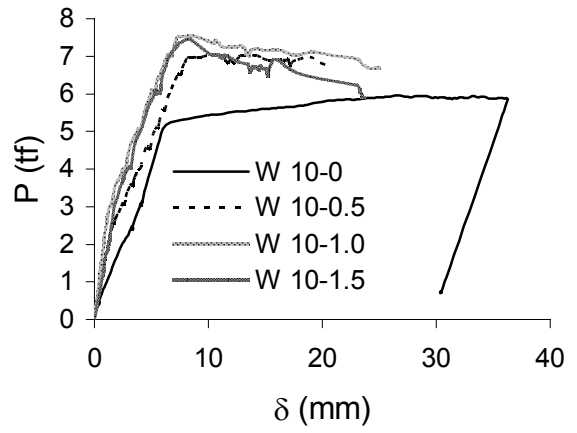


Figure 12 Load (P) – Deflection ( $\delta$ ) Curves (Series W 10)

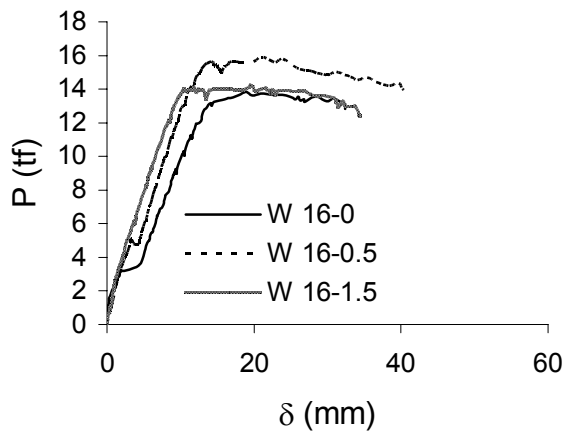


Figure 13 Load (P) – Deflection ( $\delta$ ) Curves (Series W 16)

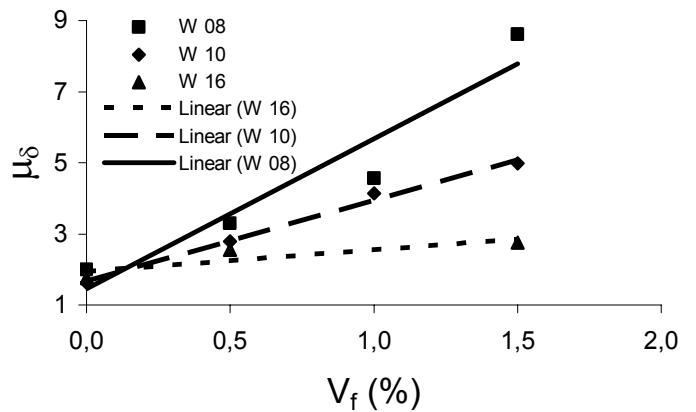


Figure 14 Influence of fibre volume on ductility index

Table 5  
Experimental results and ductility index

Wall	$A_s$ (mm <sup>2</sup> )	$V_f$ (%)	$P_y$ (kN)	$\delta_y$ (mm)	$P_u$ (kN)	$\delta_u$ (mm)	$\mu_\delta$
W 08	150	0	35.86	15.52	36.69	31.08	2.00
		0.5	41.67	5.96	41.83	19.66	3.30
		1.0	45.15	3.56	54.45	16.26	4.57
		1.5	35.03	2.28	49.30	19.62	8.61
W 10	236	0	58.48	22.28	59.64	36.30	1.63
		0.5	64.91	7.40	70.55	20.68	2.79
		1.0	67.99	6.04	75.36	25.00	4.14
		1.5	65.74	5.94	74.53	19.56	4.98
W 16	603	0	135.00	17.18	138.40	30.09	1.75
		0.5	149.68	12.64	159.19	32.28	2.55
		1.0	100.43	6.64	141.00	-	-
		1.5	137.12	10.02	141.76	27.68	2.76

The ultimate points were determined according to the previously noted criterion. For wall W 16, with  $V_f = 1.0\%$ , it was not possible to draw the  $P - \delta$  curves on their final part, due to problems with data acquisition.

Table 5 also presents the experimental results for the deflection ductility index ( $\mu_\delta$ ). From Table 5, it can be seen that as the fibre volume increases in series W 08, the ductility of the walls also increases considerably.

Figure 14 shows the fibre contribution to the walls' ductility by plotting  $\mu_\delta - V_f$  graphs for all the series of walls. From Figure 14 it is noticeable that the fibre contribution is more important for walls with low reinforcement ratios (series W 08 and W 10). For series W 16, the increase of fibre volume does not modify the ductility significantly. In fact, in this series the failure always occurred by masonry compressive crushing (fragile failure).

In order to assure energy dissipation capacity in seismic zones, it is considered acceptable and adequate for masonry structures to have a minimum deflection ductility index of 4 [21]. The walls in series W 08 and W 10, with fibre volume of 1.0 and 1.5%, attained this minimum value requirement with the deflection ductility index defined in this work.

## 5. CONCLUSIONS

The self-compactability of steel fibre reinforced concrete infill can be obtained for fibre volumes up to 1.5% with the steel fibre used in this study (DRAMIX ZP 306). This conclusion is important because the ability of the concrete infill in the masonry to fill the masonry voids must be guaranteed. The tests performed on reinforced walls in this study showed the significant contribution of the steel fibre proportion in concrete infill. The fibre contribution as equivalent tensile reinforcement is considerable. The increase of flexural strength, when failure occurs by the steel bar reinforcement (ductile failure), as for the walls of series W 08 and W 10, is about 25% to 105%, according to the proportion of fibre used.

The ductility of the walls is also increased by the contribution of steel fibres. This increase is more important to the walls with low steel ratio (walls of series W 08 and W 10). The increase of fibre volume does not modify significantly the results of series W 16, the failure of which occurred by masonry crushing in the compressive zone (fragile failure).

Based on the experimental results obtained in this study, it can be concluded that the use of steel fibres in concrete infill for masonry walls is a viable solution. The improvement to the ultimate mechanical behaviour is demonstrated, namely for the ultimate strength and ductility. Therefore, this solution can be used, for example, for strengthening and consolidation purposes in structural masonry walls.

## REFERENCES

1. SHAH, S.P and BASTON G.B. "Fiber reinforced concrete: properties and applications", SP-105, American Concrete Institute, Detroit, 1987.
2. OKAMURA, H. "Self-compactability high performance concrete", ACI Concrete International, 19, 1997, pp 50-54.
3. CAMPION M.J. and JOST P. "Self-compacting concrete", Concr. Int.: Design and Construction 22 (4) (1999) 31– 34.
4. AMBROISE, J., ROIS, S. and PERA, J. "Properties of self-levelling concrete reinforced by steel fibres", Proceedings of the Third International RILEM Workshop on High Performance Fibre Reinforced Cement Composites, Edited by H.W. Reinhardt and E. Naaman, Germany, 1999, pp. 9-17.
5. GROTH, P. and THUN, H. "Influence of steel fibre reinforcement on the workability of self-compacting concrete," Concrete Science and Engineering, 2, June 2000, pp. 65-70.
6. GRÜNEWALD, S. and WALRAVEN, J.C. "Parameter-study on the influence of steel fibres and coarse aggregate content on the fresh properties of self-compacting concrete," Cement and Concrete Research, 31, 2001, pp. 1793-1798.
7. OLIVEIRA, L.A.P., GOMES, J.P.C., NEPOMUCENO, M.C.S. and PERICÃO, M.S.G. "Use of fibre reinforced self - compacting concrete for improving the strength and ductility of masonry constructions," Report 36035IECM/2000, University of Beira Interior, Covilhã, Portugal, 35 pp.
8. COUNCIL FOR MASONRY RESEARCH. "Research needs of masonry materials and systems", Research Needs Report, The Masonry Society, 1996.
9. EN 1996-1-1 - Eurocode 6 - "Design of masonry structures. Part 1-1: General rules for reinforced and unreinforced masonry," CEN, 2005.
10. EN 772-1 "Method of test for masonry units- Part 1: Determination of compressive strength". CEN, 2000.
11. EN 772-8 "Method of test for masonry units - Part 8: Determination of water absorption of aggregate concrete masonry units by soaking". CEN, 2000.
12. EN 1015. Methods of test for mortar for masonry – Part 1: Determination of flexural and compressive strength of hardened mortar, CEN, 1999.
13. Dramix, "Product data sheet," NV Bekaert S.A., 2002.
14. NP EN 12390-3. "Testing hardened concrete: Part 3 – compressive strength of test specimens" IPQ, 2003, Portugal.
15. RILEM TC 162-TDF Committee, "Test and design methods for steel fibre reinforced concrete: Recommendations for  $\sigma - \epsilon$  design method," Materials and Structures, RILEM, 33, 2000, pp. 75-81.
16. RILEM TC 162-TDF Committee, "Test and design methods for steel fibre reinforced concrete: Bending Test. Final recommendation," Materials and Structures, RILEM, 35, 2002, pp. 579-582.
17. RILEM TC 162-TDF Committee, "Test and design methods for steel fibre reinforced concrete.  $\sigma - \epsilon$  design method. Final recommendation". Materials and Structures, RILEM, 36, 2003, pp. 560-567.
18. VANDEWALLE, M. 1994, "Tunnelling the World," Zwevegem: NV Bekaert S.A.
19. SHIN, S.-W., KAMARA, M. and GHOSH, S.K. "Flexural ductility, strength prediction, and hysteretic behavior of ultra-high-strength concrete members," SP 121-13, High-Strength Concrete, Second International Symposium, Weston T. Hester, ACI, 1990.
20. BERNARDO, L.F.A. and LOPES, S.M.R. "Flexural ductility of high-strength concrete beams", Structural Concrete, Journal of the fib, 4, (3), 2003, pp. 135-154.
21. PRIESTLEY, M. "Seismic design of concrete masonry shear walls," ACI Journal, 83, January-February, 1986, pp. 58-68.